Evaporative Cooling of ^{87}Rb with Microwave Radiation

Christian Prosko
Department of Physics, University of Alberta, Edmonton, Alberta, Canada T6G 2E1
(Dated December 3, 2015)

An evaporative cooling system is employed via microwave radiation, incident on ^{87}Rb contained in a magnetic quadrupole trap, to drive transitions in the atomic vapor between trapped and untrapped states. In addition, the degree of sample losses due to these transitions is studied with consideration given to the amplitude and frequency of incident electromagnetic fields. To understand the underlying physics of evaporative cooling, a brief introduction to modern cooling techniques and theory is given.

I. INTRODUCTION

Ultracold atoms posess a plethora of interesting characteristics, warranting the torrent of recent investigation into the subject. For example: superfluids exhibit zero viscosity, while superconducters have no electrical resistance and expel magnetic field lines. Another instance of this is Bose-Einstein condensation (BEC), existing at low enough temperatures such that every particle within a boson gas 'condenses' into the quantum ground state. Such an exotic state of matter is characterized by a minimal deviation of the sample's velocity distribution, so that the Heisenberg Uncertainty Principle necessitates a large spread in the wave-function of every boson. This constitutes an intrinsically quantum mechanical state, that is, a gas of entangled bosons describable only by a single multi-particle wave-function.

The challanges inherent in reaching the low-temperature limit of quantum degeneracy, wherein a sample's DeBroglie wavelength is on the order of the inter-particle spacing, is illustrated in the gap between the discovery of superconductivity in 1911 at 4 Kelvin [1] and the first Bose-Einstein condensate observed in a dilute gas of ^{87}Rb at 170nK, eighty-four years later [2]. Doppler cooling proved an effective method for bringing the temperature of atomic vapors down to microkelvin temperatures, but further cooling was impossible without another method.

Thusly, we design and implement an apparatus for the purpose of cooling a gas of ^{87}Rb from this limit down to the nanokelvin range. One of the most popular methods of doing so, and the one utilized here, is that of evaporative cooling using microwave radiation. Just as blowing on a cup of coffee tends to cool it by allowing the hottest water molecules to evaporate, this method hinges on providing a sort of 'exit route' for the hottest atoms in a trap, while holding on to the colder atoms.

II. THEORY & METHODOLOGY

A. Doppler Cooling

Consider monochromatic laser light of frequency ω, incident on an effectively non-interacting atomic gas, carrying momentum $\hbar\vec{k}$. If one of these atoms has velocity $\vec{v}$, then in said particle's rest frame, the light is Doppler-shifted to frequency $\omega_D = -\vec{k}\cdot\vec{v}$. Due to the discretization of electronic energy levels, a photon may transfer its momentum to the atom only if its energy $E_{ph} = \hbar\omega$ so that its frequency is in resonance with one such level. The Doppler shifting described above, however, makes this resonance dependent on the atomic velocity.

It is thus clear how lasers may be applied to reduce gas temperature. If a laser is tuned to just below a transition energy, it will only transfer its momentum to atoms travelling in the *opposite* direction of light propagation. Multiple pairs of opposing lasers directed radially inward toward a sample could then be made to reduce the average kinetic energy of a sample [3, p. 73-122].

Unfortunately, Doppler cooling has a limit. The effect of spontaneous emission of photons is on average isotropic, so that no net momentum is imparted to the gas through this process. On the other hand, it increases the mean square velocity of constituents, and thus imparts heat to the sample. At the Doppler temperature T_D, given by [3, p. 57]:

$$T_D = \frac{\hbar\gamma}{2k_B} \tag{1}$$

the cooling effect is overwhelmed by spontaneous emission[1]. Here γ is the natural linewidth of the excited

[1] Some more complicated laser cooling methods such as Sisyphus cooling [4] use an optical polarization gradient to cool below this limit, but they still have limits above the temperature range for quantum degeneracy around the recoil temperature: $T_r = (\hbar k)^2/(2k_B M)$.

state, *i.e.* the reciprocal of the excited state's typical lifetime. Generally, this limit is on the order of $100\mu K$; this is several orders of magnitude above the temperature required for BEC. Hence, we are motivated to study a complementary method of cooling utilizing microwave radiation.

B. Magnetic Trapping of Neutral Atoms

As a result of the Zeeman effect, a magnetic field $\vec{B}$ introduces a term $\hat{H}_m = -\hat{\mu} \cdot \vec{B}$ ($\hat{\mu}$ being the magnetic dipole operator) to the single-atom Hamiltonian, resulting in a splitting of hyperfine energy levels. For alkali atoms which have a single valence electron in an s-orbital, hydrogenic quantum states are effective in describing their properties, since they may be approximated as a heavy nucleus of $+e$ charge surrounded by a single electron. In a state with zero orbital electron momentum these splittings ΔE_F may be calculated from the Breit-Rabi formula, as derived in Appendix A:

$$\Delta E_{|F=I\pm 1/2, m_F\rangle} = -\frac{\Delta E_{hf}}{4(I+1/2)} + \mu_B g_I m_F B \pm \frac{\Delta E_{hf}}{2}\sqrt{1+\frac{2m_F x}{I+1/2}+x^2} \quad (2)$$

In which $x \equiv \frac{g_J \mu_B B}{\Delta E_{hf}}$, ΔE_{hf} denotes the hyperfine energy gaps in the absence of an external magnetic field, g_I, g_J, and g_F are Landé g-factors[2], and $m_F \in \{-F, -F+1, ..., F-1, F\}$ is the magnetic quantum number. Energy splittings calculated for ^{87}Rb from this formula are plotted in Figure 1.

The most important consequence of eq. (2) is that certain states have a lower energy in higher magnetic fields, whereas other $|F, m_F\rangle$ states seek lower magnetic field strength to minimize their energy or are unaffected by this added potential. Thusly, a magnetic field with a region of minimum strength may trap 'high-field seeking' states, while allowing others to escape (see Figure 1).

This is more readily apparent in the weak-field limit of Zeeman splittings, where the static field may be treated as a small perturbation of the fine structure Hamiltonian for which $|F, m_F\rangle$ are the eigenstates. The first order energy correction is then:

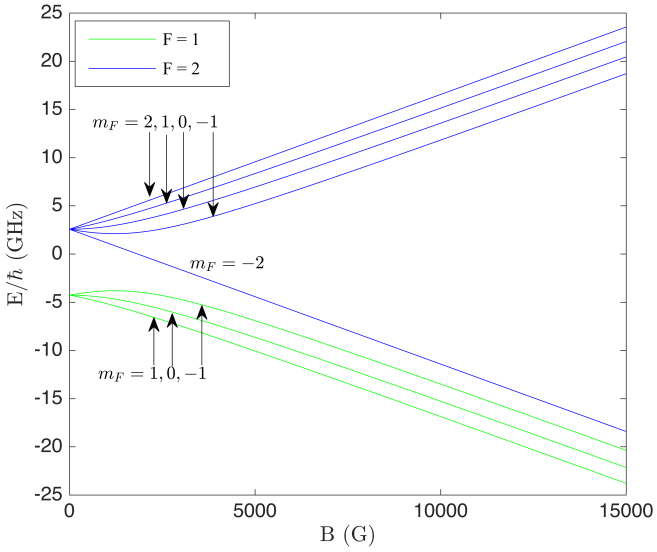

FIG. 1. Ground-state energy splitting of hyperfine levels in ^{87}Rb in the presence of a uniform magnetic field, calculated from the Breit-Rabi formula.

$$\begin{aligned}\Delta E_{|F,m_F\rangle} &= \langle F, m_F| \hat{\mu} \cdot \vec{B} |F, m_F\rangle \\ &= \langle F, m_F| \left(\frac{g_F \mu_B}{\hbar}\right) \hat{F} \cdot \vec{B} |F, m_F\rangle \\ &= \frac{g_F \mu_B B}{\hbar} \langle F, m_F| \hat{F}_z |F, m_F\rangle \\ &= g_F \mu_B m_F B \end{aligned} \quad (3)$$

noting that $g_F = -1/2, 1/2$ for $F = 1, 2$ respectively, and that $\hat{z}$ is the axis of quantization *i.e.* the direction of $\vec{B}$. This is an application of the theorem which states that if degenerate eigenfunctions of an unperturbed Hamiltonian $\hat{H}_0$ are also eigenfunctions with *distinct* eigenvalues of a Hermitian operator $\hat{A}$ which commutes with both $\hat{H}_0$ and the perturbation $\hat{H}'$, then the first order energy correction is the same as that from non-degenerate perturbation theory. In this case, $\hat{A} = \hat{F}_z$, which commutes with the fine structure Hamiltonian and (on time average) with $\hat{H}_m$ [5, p. 277].

To achieve the sort of trapping field described previously, a magnetic quadrupole trap is used. By assembling three Helmholtz pairs along perpendicular axes, a magnetic field is established with a region in the center of the form[3]:

[2] These are constants for a given isotope corresponding to nuclear spin I, total electron angular momentum $J = L + S$ (where L and S are orbital and spin angular momentum for the valence electron), and total atomic angular momentum $F = I + J$.

[3] The factor of 2 in the z-component is necessitated by Maxwell's equation: $\vec{\nabla} \cdot \vec{B} = 0$. We use this to our advantage, pointing the $\hat{z}$-axis vertically to reduce any gravitational effects on our sample.

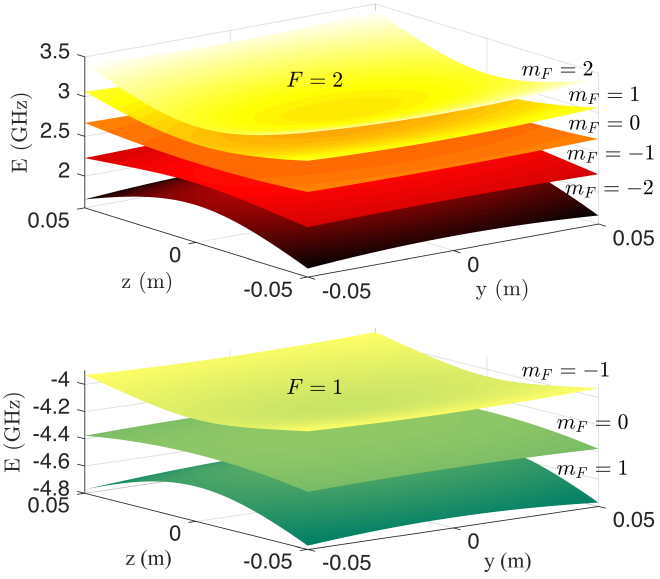

FIG. 2. Hyperfine energy levels in a linear magnetic field: $\vec{B} = (0.5\text{Tm}^{-1})(x\hat{x} + y\hat{y} - 2z\hat{z})$ at constant $x = 5\text{cm}$.

$$\vec{B} = B_0(x\hat{x} + y\hat{y} - 2z\hat{z}) \tag{4}$$

Substituting this field into eq. (2), we find that $\vec{r} = 0$ is either a minimum or maximum in potential energy depending on the magnetic quantum number (see fig. 2).

This sort of magnetic trapping scheme has a significant downside, however. At the point where magnetic field strength vanishes, the Zeeman energies beome degenerate, making the spin (*i.e.* m_F value) ambiguous. Once the atom reemerges into a region of non-zero magnetic field, its spin may have flipped in what is called a 'Majorana transition' [6]. These transitions occur frequently enough that resulting particle losses inhibit trap lifetime to a detrimental degree. In addition, the experiments possible in a magnetic trap are limited outside of Bose-Einstein Condensation, since whether an atom is held in the trap or not is fundamentally dependent on the internal (hyperfine) atomic state.

For these reasons, magnetic quadrupole traps are generally supplemented with a perturbative light source to create a bias in the magnetic field zero. A common example of this is a time-oscillating magnetic field designed to translate the zero-point around in a circle. For frequencies greater than the atomic orbital frequency around the field zero, low-field seeking atoms 'follow' the zero-point without reaching it, effectively eliminating the possibility of spin-flip transitions [7].

Another such preventative technique – the one used by this group – is an optical dipole trap directed about the magnetic trap minimum. These traps have been well established and described (for example, see: [3, 8]), and operate by using lasers to simultaneously induce an oscillating electric dipole moment in atoms, whilst using the resulting dipole force to pull the atoms to the region where laser light is most focused (this is called the beam waist). This force results from a gradiant in the Stark shift[4] due to spatial variation in the intensity of focused light. As a result, atoms are trapped in the vicinity of the beam waist, where the electric field gradient is strongest. In conjunction with a magnetic quadrupole trap, optical dipole traps can produce shallow minima in potential energy surrounding the point of zero magnetic field, encouraging trapped atoms to avoid the point of vanishing field strength.

C. Rabi Flopping

Evaporative cooling relies on electromagnetic radiation to instigate transitions between magnetic sublevels in atoms, so it is worth discussing the manner in which a monochromatic light source accomplishes such a task. In general, Rabi Flopping describes a system's evolution between two otherwise stationary states as a result of a perturbative time-oscillating potential[5]. In our case, we approximate the unperturbed system as being a rubidium atom confined to an approximately uniform region of the magnetic trapping field, driven to oscillate between $F = 1$ and $F = 2$ states by a linearly polarized magnetic wave $\vec{B}^{mw}$ of microwave frequency near the $\omega_0 \equiv 6.834\text{GHz}$ transition [11]. The trapping field defines a quantization axis (say, along the $\hat{z}$ axis) and thus creates a magnetic dipole moment $\hat{\mu} = \hat{\mu}_I + \hat{\mu}_S + \hat{\mu}_L$, so that the perturbative potential is:

$$\hat{V} = \vec{\mu} \cdot \vec{B}^{mw} = (\hat{\mu}_I + \hat{\mu}_S) \cdot \vec{B}^{mw} \tag{5}$$

in the ground state of rubidium ($L = 0$). Before continuing, it is worth noting that since the trapping field's directionality varies with position, microwave radiation will have a distinctly varying effect at certain regions in the trap. In particular, when $\hat{z}$ happens to be exactly parallel or perpendicular to $\vec{B}^{mw}$. This implies that

[4] The energy shifting effect of electrons being pulled in the opposite direction as the positive nuclei in an electric field.

[5] Most graduate quantum physics texts cover this topic; see for example: [3, 9, 10].

any usage of microwaves to manipulate energy states of trapped atoms requires a consideration of the system's geometry. Since evaporative cooling relies on transitions from trapped to untrapped states, only the $|2,2\rangle \leftrightarrow |1,1\rangle$ and $|2,1\rangle \leftrightarrow |1,1\rangle$ transitions are relevant to our discussion[6]. Thusly, we suppose $\vec{B}_{mw} = B^{mw}\cos(\omega t)\hat{x}$ is perpendicular to the trapping field in some region, so:

$$\hat{V} = \frac{\mu_B B^{mw}}{\hbar}(g_I \hat{I}_x + g_S \hat{S}_x)\cos\omega t \tag{6}$$

Obviously, this is not a two-state system in the $|F, m_F\rangle$ basis, but considering the case of a $|2,2\rangle \rightarrow |1,1\rangle$ transition, where the microwaves are turned on at $t = 0$ and remain on, we may say that the general quantum state for $t < 0$ is $|\psi\rangle = c_1|1,1\rangle + c_2 e^{i\omega_0 t}|2,2\rangle$ since both states are eigenstates of the unperturbed Hamiltonian. Here we have shifted our zero energy such that $E_1 = 0$ and $E_2 = \hbar\omega_0$. After $\hat{V}$ is introduced at $t = 0$, we assume that our state is invariant except for a time dependence granted to the previously constant coefficients c_1 and c_2. The Schrödinger equation then yields:

$$\begin{pmatrix} c_1'(t) \\ c_2'(t)e^{i\omega_0 t} \end{pmatrix} = \frac{e^{i\omega t} + e^{-i\omega t}}{2i}\begin{pmatrix} 0 & \Omega \\ \Omega & 0 \end{pmatrix}\begin{pmatrix} c_1(t) \\ c_2(t)e^{i\omega_0 t} \end{pmatrix} \tag{7}$$

where $\Omega \equiv \langle 2,2|\hat{V}|1,1\rangle/(\hbar\cos(\omega t))$ is a constant called the Rabi Frequency. Note that one of the time derivative terms cancels the unperturbed Hamiltonian terms, and that the diagonal potential terms are 0 [12]. Clearly, for near-resonance $\omega \approx \omega_0$, some terms oscillate at almost twice ω_0, while others oscillate very slowly (frequency $\omega_0 - \omega$). We thus make the rotating wave approximation: That these rapidly oscillating terms are neligible [13]. Then:

$$i\hbar\begin{pmatrix} c_1'(t) \\ c_2'(t) \end{pmatrix} = \begin{pmatrix} 0 & \frac{1}{2}\Omega \\ \frac{1}{2}\Omega & 0 \end{pmatrix}\begin{pmatrix} c_1(t) \\ c_2(t) \end{pmatrix} \tag{8}$$

Solving for one coefficient in either equation, differentiating the other and substituting in the result, we have:

$$c_1''(t) - i(\omega_0 - \omega)c_1'(t) + \frac{1}{4}\Omega^2 c_1(t) = 0 \tag{9a}$$

$$c_2''(t) + i(\omega_0 - \omega)c_2'(t) + \frac{1}{4}\Omega^2 c_2(t) = 0 \tag{9b}$$

with $\gamma \equiv \omega_0 - \omega$ being the frequency detuning. This differential equation can be solved analytically, simply by choosing integration factors such that $c_1(t) = b_1(t)e^{\frac{1}{2}i\gamma t}$ and $c_2 = b_2(t)e^{-\frac{1}{2}i\gamma t}$ for some functions $b_1(t), b_2(t)$. Our differential equations then become:

$$b_1''(t) - \frac{1}{2}i\gamma b_1'(t) + \frac{1}{4}(\gamma^2 + \Omega^2)b_1(t) = 0 \tag{10a}$$

$$b_2''(t) + \frac{1}{2}i\gamma b_2'(t) + \frac{1}{4}(\gamma^2 + \Omega^2)b_2(t) = 0 \tag{10b}$$

These equations are merely those for simple harmonic oscillators, and have general solutions of the form $A\sin\Omega' t + B\cos\Omega' t$, where one coefficient is constrained by the first derivative term and $\Omega' \equiv \frac{1}{2}\sqrt{\Omega^2 + \gamma^2}$. Supposing our system is initially prepared in the $|2,2\rangle$ state such that $c_1(0) = 0$ and $c_2(0) = 1$, these constraints in addition to the total probability condition $|c_1|^2 + |c_2|^2 = 1$ provide the final solution:

$$c_1(t) = -i\frac{\Omega}{\Omega'}\sin(\Omega' t)e^{-\frac{1}{2}i\gamma t} \tag{11a}$$

$$c_2(t) = \left[\cos(\Omega' t) - i\frac{\Omega}{\Omega'}\sin(\Omega' t)\right]e^{\frac{1}{2}i\gamma t} \tag{11b}$$

Qualitatively, the most important consequences of this result are that detuned light may still initiate transitions between levels (albeit with lower probability), and the probability of finding a particle in $|2,2\rangle$ or $|1,1\rangle$ oscillates with frequency Ω'. The value of Ω has been calculated in [12][7] and in Appendix B, so that the frequency of oscillation between states is:

$$\Omega' = \frac{1}{2}\sqrt{(5.81945\cdot 10^{21}\mathrm{Hz}^2/\mathrm{T}^2)B^{mw^2} + \gamma^2} \tag{12}$$

D. Evaporative Cooling

Finally, we are prepared to discuss evaporative cooling. Supposing all or most of the atoms in a Rubidium-87

[6] Transitions between m_F levels at constant F can also untrap atoms, but the corresponding transition frequencies are far below the microwave range. Radio-frequency evaporative cooling, for example, uses such transitions.

[7] This calculation involves expanding $|F, m_F\rangle$ states in terms of $|m_I, m_J\rangle$ states and calculating the expectation value using Clebsch-Gordan coefficients. $\hat{\mu}_I$ is neglected in [12], but this is reasonable since $g_I \approx -0.001$ is several orders of magnitude smaller than $g_S \approx 2$ [11].

sample have been prepared and magnetically trapped in the $|F, m_F\rangle = |2, 2\rangle$ state, (say, via optical pumping [14]) and that a microwave source of tunable frequency near the 6.834GHz transition from $F = 2 \rightarrow F = 1$ is incident upon the magnetically trapped atoms. Only the $|2, 2\rangle \rightarrow |1, 1\rangle$ transition can untrap these atoms whilst also lying in the microwave range of transition frequencies. In fact, this is the *only* possible transition from $|2, 2\rangle$ that could be driven by microwave frequencies, since transitions involving $\Delta m_F > 1$ are impossible regardless of the directionality relation between $\vec{B}^{mw}$ and the static field on account of quantum selection rules (see [3, p. 49]).

With knowledge of the theory considered in sections II B and II C, the principles behind evaporative cooling are in fact quite simple. In general, atoms trapped in the $|2, 2\rangle$ state near the center of a magnetic quadrupole trap have increasing energy with distance from the magnetic field's minimum strength region. Microwaves detuned a small frequency γ above the zero-field 6.834GHz transition will interact only with atom's whose Zeeman splittings are large enough to reach the transition energy corresponding to this raised frequency. This creates an effective 'edge' to the trap, since atoms distanced farther from the trap center are in higher magnetic fields, and given enough kinetic energy may continue travelling until their Zeeman splittings are resonant with $\hbar\gamma$ transitioning them to an untrapped state. This is key: only the atoms with enough kinetic energy, *i.e.* the *hottest* atoms, are able to move into high enough fields to be freed from the trap. It is easy to see, then, where this cooling technique's name comes from; perspiration, for example, involves especially the hottest sweat evaporating into air, carrying excess heat away and cooling the skin.

Keeping this in mind, the general procedure for evaporative cooling is as follows: Microwaves propagating through the quadrupole trap are tuned to high enough frequencies so as to only remove the highest temperature trapped atoms. After rethermalizing, the remaining sample's temperature has been lowered. Repeating this procedure at progressively lower frequencies can, in theory, lower the temperature indefinitely [15].

In reality, this procedure is limited by multiple factors. Firstly, the collision rate between particles is approximately $n\sigma v_T$ where n is number density, σ is the collision cross section, and $v_T = \sqrt{8k_BT/(\pi M)}$ is the mean particle speed according to a Maxwell-Boltzmann distribution. As this rate decreases proportionally to $T^{1/2}$, the rethermalization rate becomes slower and slower as the sample is cooled. This, combined with the limited lifetime of a trapped sample, is a hindrance to reaching quantum degeneracy temperatures. As a magnetic field of the form in eq. (4) restricts colder atoms to move within a smaller region of space near its minimum, it has the counteracting effect of increasing density with decreasing temperature. In a well designed cooling apparatus, the latter effect may exceed the former such that rethermalization rate increases with decreasing temperature, but another effect sets a lower limit to evaporative cooling: inelastic collisions. Internal energy may be transferred between atoms in an inelastic collision, which in turn can cause transitions from trapped to untrapped states or simply an increase in an increase in one atom's speed. Overall, this gives evaporative cooling a lower bound on the order of 1nK [15].

III. EXPERIMENTAL SETUP & PROCEDURE

Initially, a vapor of ^{87}Rubidium atoms is doppler-cooled by a 2-dimensional Magneto-Optical Trap (MOT) produced by four lasers directed inward along two perpendicular axes, in conjunction with four coils used as a 2D magnetic quadrupole trap. As described in Section II A, any transfer of momentum from the laser beams to the vapor serves to cool the atoms. Another benefit of the magnetic field gradient is therefore that, in addition to trapping atoms, it serves to increase the likelihood of momentum transfer from the laser beams. This is because atoms moving outwards from the trap center may reach the resonant Doppler shift for transitions more quickly as a result of Zeeman splitting. As the trap potential and laser beams are directed only along two dimensions, the atoms retain their speed along the other perpendicular axis and are therefore focused into a beam directed towards the next stage of cooling.

A second MOT, established by three Helmholtz pairs and lasers directed along all three perpendicular axes, collects and confines the atoms in three dimensions. This is where the majority of Doppler cooling occurs. Afterwards, the magnetic trap is turned off, and optical molasses cooling[8] is performed for 18ms, then atoms are optically pumped into the $|2, 2\rangle$ state over the course of

[8] This method uses detuned lasers and the Doppler effect to create a frictional force approximately proportional to atomic velocity. Though it does not provide an equilibrium restoring force, and hence does not trap atoms, their 'molasses' like movement under this friction force allows them to be held for the duration of this process [**?**].

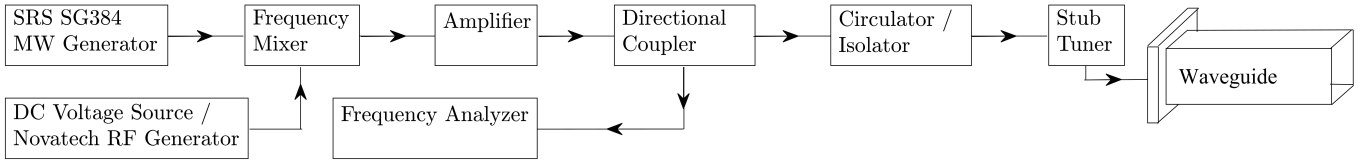

FIG. 3. Evaporative cooling apparatus. The stub tuner allows for impedance matching, optimizing power transfer to waveguide. Also, the circulator-isolator functions by permitting power transmission along one direction only, preventing interference of reflected waves with other instruments.

1.2ms. The magnetic field is turned back on, and strength is then ramped up for 1s, since the resulting higher density increases rethermalization rates in preparation for evaporative cooling.

Two primary experiments were attempted with our microwave cooling apparatus, as illustrated in Figure 3. In the former, the microwave generator was left on for the entire course of the cooling cycle. The end of the waveguide was positioned approximately 10cm from ^{87}Rb in the 3D quadrupole trap. Though it was also directed towards the 2D MOT chamber, the microwaves would have negligible interference with that stage as a result of the rapid spatial decay of electromagnetic radiation. The SG384 microwave generator was set to oscillate linearly 0.5MHz about a central frequency (at a rate of 5Hz) while the Rubidium cloud is held in the trap for 5s, then the trap was suddenly released, allowing the Rubidium cloud to expand for 3ms before capturing an image. The entire cycle was repeated 5 times for each central frequency, after which the frequency was stepped down by 1MHz and the procedure began again.

This allowed for observation of spin-flip transitions by comparing the number of atoms in the cloud after 5 seconds with no microwaves, with that after 5 seconds accompanied by a strong microwave signal. A high power signal, however, incites more complete Rabi oscillations over a wider range of frequencies (as shown in eq. (12)), and therefore is expected to destroy the trapped vapor at considerably higher frequencies than those for a low power signal. To test this, a second round of data was collected with a DC power source mixed into the microwave signal, set to low enough power to attenuate the original signal to about half its original amplitude.

To estimate the number of atoms in the cloud, absorption imaging is used. A laser tuned to a resonant transition (780nm in this case [11], from $5^2S_{1/2}$ to $5^2P_{3/2}$) passes through the trap when there are no atoms, and its intensity I_0 is measured by a camera. Another picture is then taken after the cloud expansion, and the intensity of images is compared according to the standard attenuation formula:

$$I = I_0 e^{-\sigma \int n dz} \tag{13}$$

where n is number density and σ in this case is the scattering cross section for resonant light at the 780nm transition. For distinguishable particles above 'quantum' temperatures, density is given by the Boltzmann distribution:

$$n = n_0 e^{-H/(k_B T)} \tag{14}$$

for some n_0. For a rough measure of particle number, we approximate our Hamiltonian as being that of a simple harmonic oscillator: $H \approx \frac{p^2}{2m} + \frac{1}{2} m\omega^2 r^2$ for some ω. Then the number of atoms N in the cloud is about:

$$N = \int n dx dy dz = n_0 \left(\frac{2\pi k_B T}{m\omega^2} \right)^{3/2} \tag{15}$$

Carrying out the integral in eq. (13) and substituting in the result from eq. (15), we have:

$$-\log\left(\frac{I}{I_0}\right) = \sigma N \left(\frac{m\omega^2}{2\pi k_B T}\right) e^{-(x^2+y^2)m\omega^2/(2k_B T)} \tag{16}$$

$$\equiv A e^{-(x^2+y^2)/(2\sigma_x \sigma_y)} \tag{17}$$

Thus, to measure particle number, we numerically fit the processed camera images to a Gaussian, and calculate N from the resulting amplitude and standard deviations according to:

$$N = \frac{2\pi \sigma_x \sigma_y A}{\sigma} \tag{18}$$

For the optical transition in question, $\sigma = 3\lambda^2/(2\pi) \approx 2.9 \times 10^{-13} m^{-2}$.

The second experiment was an attempt in evaporative cooling. After applying various frequency ramps, we observed the atomic cloud's size and compared it to the cloud size with a static trapping field only. This

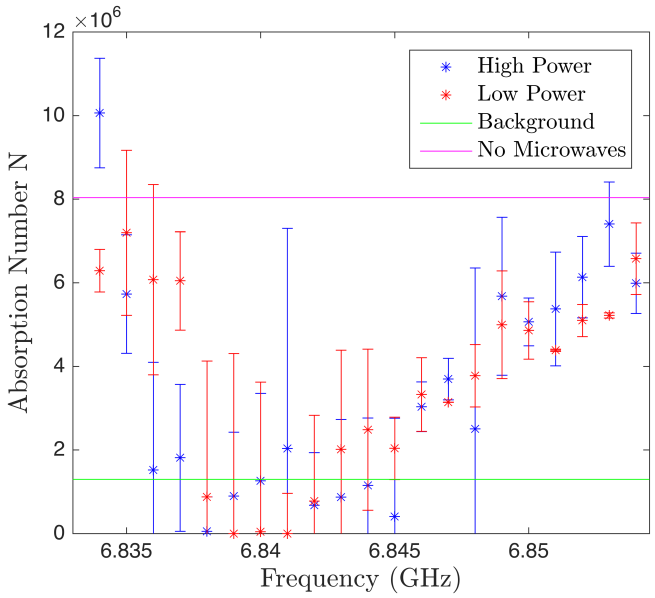

FIG. 4. Particles observed still inside trap after a time-of-flight period of 3ms, as a function of trap edge (microwave frequency). The uncertainty is approximately ±1 standard deviation across values observed at the same frequency. Background denotes what the average absorption number *would* be if eq. (15) was applied to background data (no atoms)

is because according to eq. (16), σ_x and σ_y are both proportional to $\sqrt{T}$, so that a smaller cloud is signature of lower temperature. Here, the microwave signal is mixed with a radio-frequency signal triggered precisely after the compression phase of the cycle, and turns off immediately before the cloud is allowed to expand for imaging.

IV. RESULTS

Evidenced in Figure 4, the microwave apparatus possessed more than sufficient power to transition atoms out of the trap. As expected from our discussion of Zeeman splitting, this effect increased as the microwave frequency approached resonance with the magnetically perturbed hyperfine energy levels from above, and then decreased just before the 6.834GHz limit was reached. The latter effect is expected, since the magnetic field is non-zero (almost) everywhere, so that essentially all atoms would have energies slightly shifted from the unperturbed hyperfine transition. Also, our results were too inaccurate to determine with certainty if a stronger field produced a sharper 'critical' frequency after which atoms are more rapidly removed. On the other hand, as the absorption number for the high power setup remained within error of 0 for $6.836 - 6.837$GHz, the low power setup already

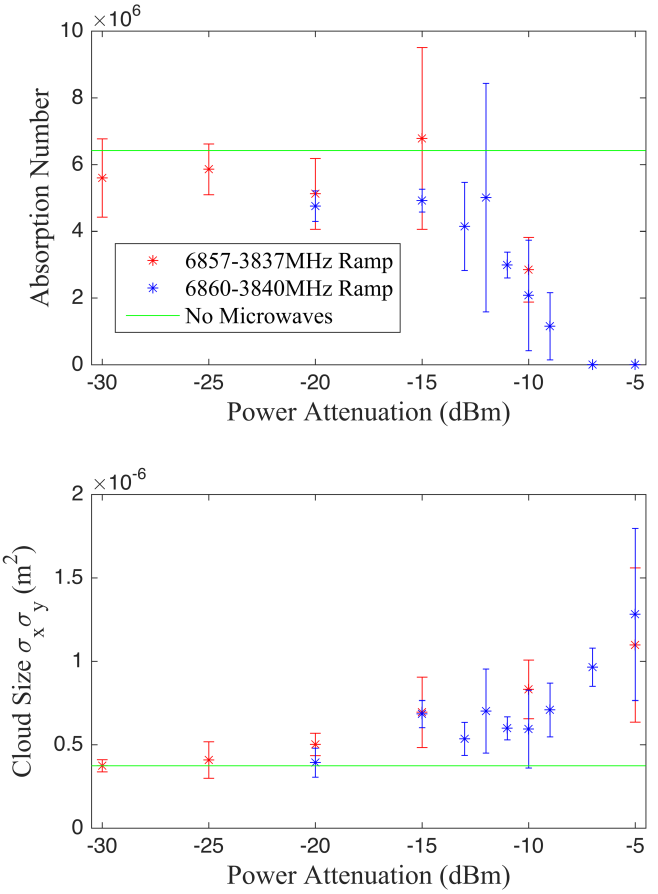

FIG. 5. Efficacy of evaporative cooling for two linear 5s ramps at various microwave amplitude levels. $\hat{x}$-axis is simply the attenuation when compared to the unmodified RF signal.

was too far detuned from resonant energies to remove the majority of atoms with these frequencies, in agreement with the amplitude dependence of transition probabilities (*i.e.* the squared coefficients from eqs. (11a) and (11b)).

Before applying our apparatus to evaporative cooling, a suitable frequency ramp should be determined with consideration of the microwaves' intensity, range, and the duration of the ramp. As such, linear ramps attenuated by controlling the amplitude of the mixed RF signal to various strengths were tried, and plotted in Figure 5. Because an evaporative cooler seeks to lower the temperature of a sample rather than eliminate its presence completely, it is inferred from the data that average powers greater than -10dBm would leave no sample behind after cooling. Next, ramp duration was varied for a single frequency range and power, with the results displayed in Figure 6. Clearly, only ramps lasting between 2 and 6 seconds were long enough to remove any atoms, while short enough to be well within the trap's lifetime. It is worth noting that, with all experiments

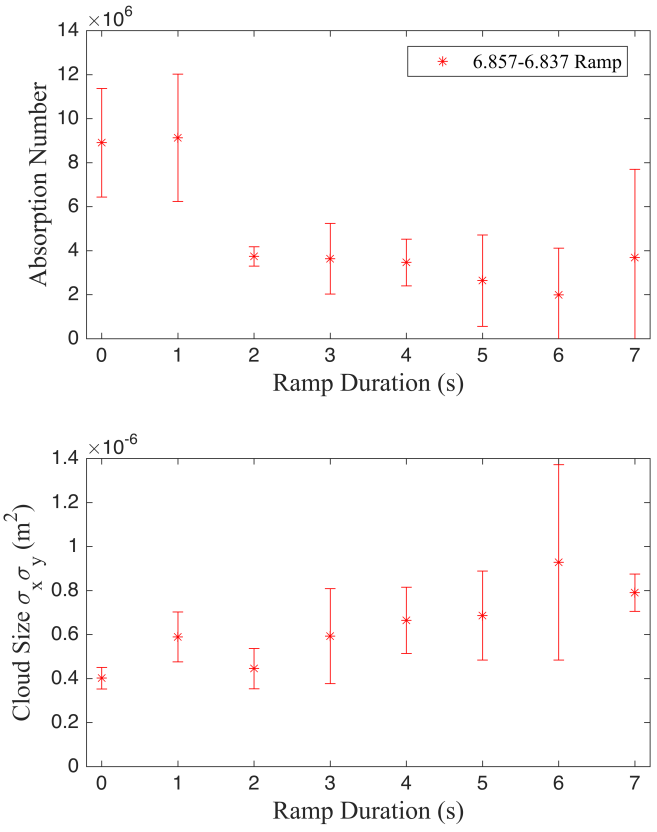

FIG. 6. Efficacy of evaporative cooling for a single linear ramp, spread over different ramp durations.

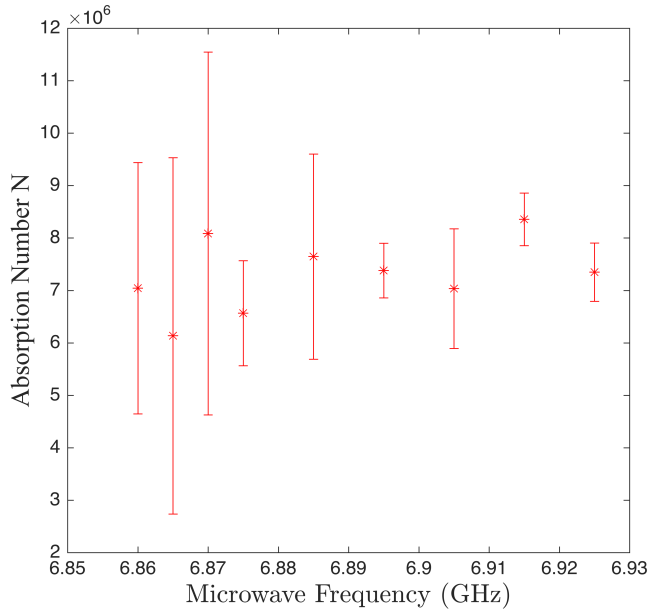

FIG. 7. The microwave frequency is lowered from frequencies far detuned from 6.834GHz, displaying no loss of atoms.

Ramp	Abs. Number N	$\sigma_x\sigma_y$ (m^2)
None, 3.5s	$(6.9 \pm 1.5) \cdot 10^6$	$(3.5 \pm 0.4) \cdot 10^{-7}$
Linear, 6.857-6.837GHz	$(3.6 \pm 1.6) \cdot 10^6$	$(5.9 \pm 2.2) \cdot 10^{-7}$
Exponential, 6.885-6.835GHz	$(6.1 \pm 2.2) \cdot 10^6$	$(3.8 \pm 1.1) \cdot 10^{-7}$

TABLE I. Efficiency of cooling for linear ramps, and a ramp with exponential decrease in frequency with respect to time. Both above ramps lasted 3.5s. Data is averaged over 10 trials for the first and last sweeps, and 5 trials for the second.

performed, uncertainty in the cloud size and absorption number becomes very large for small values of these quantities as a result of the breakdown of approximation that the vapor's density distribution is Gaussian.

Attempting evaporative cooling with different frequency ranges and shapes of ramps suggested a critical flaw in our experimental setup: the microwave ramps consistently *increased* the cloud size, apparently heating the atoms rather than cooling them. Some results are presented in Table I, though many more ramps were tested. Of course, it would be naive to assume that the optimum microwave power and frequency change rate should be the same at different frequencies, which is why 12 different ramps with step-wise exponentially decaying frequency (at various powers) were tested in addition to the 25 or so different linear ramps considered. The results for the linear ramp in table I were typical of all linear ramps attempted: All were able to effectively remove atoms while leaving a small sample behind, though the atomic vapor was heated in the process.

The exponentially decaying ramp is shown because it is the only tested frequency sweep which at least maintained a cloud size comparable to that of a pure magnetic trap in the absence of microwaves, while still removing a significant number of atoms. To be precise, this ramp consisted of 500ms going from 6.885-6.855GHz, 500ms from 6.855-6.845GHz, 500ms from 6.845-6.84GHz, and finally 2s sweeping from 6.84-6.835GHz. The amplitude of its RF-signal was set at each step to -10dBm, -15dBm, -15dBm, and -20dBm, respectively. Its upper frequency was determined by lowering the frequency from far above ω_0 until the absorption number slightly decreased (see fig. 7).

Unfortunately, none of these optimization efforts revealed what was adding thermal energy to the system, preventing evaporative cooling from being observed. It is possible, however, that one source of heating is interference of the unmixed microwave signal with the trapped atoms. The microwave generator was set to 6.825GHz for the ramping experiments, a frequency that may not have been detuned enough from 6.834GHz to prevent interactions with the trap. Though the mixer used weakens the unmixed signal, it still remained at more than 50% percent of the mixed signal's amplitude, as measured by a frequency analyzer tapped into the circuit through a directional coupler. On the other hand, absorption numbers observed with the frequency ramp turned off are in the same range as those with the ramp turned on, but with a high cutoff frequency. If any atoms were leaking through this possible 'hole' in the trap, there were unmeasurably few. Nonetheless, colder atoms are more likely to be located near the trap minimum, where the 6.825GHz signal is least detuned from Zeeman split energies. Thus, it is possible that a sort of reverse evaporative cooling was occurring, with primarily the coldest atoms escaping the trap through this interaction.

V. CONCLUSION

The intrinsically quantum mechanical effects of oscillating magnetic fields on atomic angular momentum were demonstrated by utilizing microwaves to 'flip' ^{87}Rb atoms from magnetically trapped total angular momentum states to untrapped states. These observations are explained by weak-coupling perturbation theory of a magnetic field with magnetic sublevels of the atoms. Unfortunately, an unforeseen heating mechanism prevented the observation of evaporative cooling, although lowering the frequency of the unmixed microwave signal could remedy this.

Appendix A: Derivation of the Breit-Rabi Formula

If an alkali atom is in its fine structure ground state such that $L = 0$, $J = {}^1\!/_2$, and $I = {}^3\!/_2$, the most complete hydrogenic basis states are $|m_I, m_J\rangle$. Under these conditions, the unperturbed Hamiltonian is effectively the hyperfine coupling between electron and nuclear angular momentum, for which $|F, m_F\rangle$ are eigenstates:

$$\hat{H} = A\hat{I}\cdot\hat{J} + (\hat{\mu}_I + \hat{\mu}_J)\cdot\vec{B} \tag{A1}$$

where A is an energy constant for a given isotope and L level. Using the standard ladder operators $\hat{Q}_\pm \equiv \hat{Q}_x \pm i\hat{Q}_y$, we may rewrite this as:

$$\begin{aligned}\hat{H} &= A(\hat{I}_x + \hat{I}_y + \hat{I}_z)\cdot(\hat{J}_x + \hat{J}_y + \hat{J}_z) + \mu_B B(g_I\hat{I}_z + g_J\hat{J}_z)\\ &= A\left[\hat{I}_z\hat{J}_z + \left(\frac{\hat{I}_+ + \hat{I}_-}{2}\right)\left(\frac{\hat{J}_+ + \hat{J}_-}{2}\right)\right.\\ &\quad\left. + \frac{i}{2}(\hat{I}_- - \hat{I}_+)\frac{i}{2}(\hat{J}_- - \hat{J}_+)\right] + \mu_B B(g_I\hat{I}_z + g_J\hat{J}_z)\\ &= A\left[\hat{I}_z\hat{J}_z + \frac{1}{2}(\hat{I}_+\hat{J}_- + \hat{I}_-\hat{J}_+)\right] + \mu_B B(g_I\hat{I}_z + g_J\hat{J}_z)\end{aligned} \tag{A2}$$

In this system, m_F is conserved such that $m_F = m_I + m_J$. Any suspicion towards the seemingly classical treatment of the dipole moment dot product with $\vec{B}$ is well founded, as $\hat{I}$ and $\hat{J}$ dipole moments are in general precessing about the quantization axis in possibly different directions. This is called 'Larmor Precession,' and its behaviour is accounted for by the g-factors. Thus, we approximate the perturbed energies by diagonalizing the Hamiltonian's matrix form in the $|m_J = \pm{}^1\!/_2, m_I = m_F \mp {}^1\!/_2\rangle \equiv |\pm\rangle$ basis. Its elements are calculated below for given m_F:

$$\begin{aligned}\langle\pm|\hat{H}|\pm\rangle &= A\langle\pm|\hat{I}_z\hat{J}_z|\pm\rangle\\ &\quad + \frac{A}{2}\left[\langle\pm|\hat{I}_+\hat{J}_-|\pm\rangle + \langle\pm|\hat{I}_-\hat{J}_+|\pm\rangle\right]\\ &\quad + \mu_B B\left[g_J\langle\pm|\hat{J}_z|\pm\rangle + g_I\langle\pm|\hat{I}_z|\pm\rangle\right]\\ &= Am_Jm_I + \frac{A}{2}[0+0] + \mu_B B[g_Jm_J + g_Im_I]\\ &= A(\pm{}^1\!/_2)(m_F \mp {}^1\!/_2) + \mu_B B\left[\pm\frac{1}{2}g_J + (m_F \mp \frac{1}{2})g_I\right]\\ &= -\frac{A}{4} \pm \frac{Am_F}{2} + \mu_B Bg_Im_F \pm \frac{\mu_B B}{2}(g_J - g_I)\end{aligned} \tag{A3}$$

We have used the the property that $\hat{Q_\pm}|Q, m_Q\rangle = \sqrt{Q(Q+1) - m_Q(m_Q \pm 1)}\,|Q, m_Q \pm 1\rangle$ returns 0 when $|m_Q|$ would exceed Q as a result. No $\hbar$ appears upon taking inner products simply because it is contained in the definitions of A and μ_B. Similarly, for $\langle\pm|\hat{H}|\mp\rangle$:

$$\begin{aligned}\langle+|\hat{H}|-\rangle &= \frac{A}{2}\left[\langle+|\hat{I}_+\hat{J}_-|-\rangle + \langle+|\hat{I}_-\hat{J}_+|-\rangle\right]\\ &= \frac{A}{2}\left[0 + \sqrt{(I + m_F + {}^1\!/_2)(I - m_F + 1 - {}^1\!/_2)}\right.\\ &\quad\left.\times\sqrt{({}^1\!/_2 + {}^1\!/_2)({}^1\!/_2 - {}^1\!/_2 + 1)}\right]\\ &= \frac{A}{2}\sqrt{(I - m_F + {}^1\!/_2)(I + m_F + {}^1\!/_2)}\\ &= \frac{A}{2}\sqrt{(I + {}^1\!/_2)^2 - m_F^2}\end{aligned} \tag{A4}$$

which is also the expression for $\langle -|\,\hat{H}\,|+\rangle$ since $\hat{H}$ is Hermitian. Thus, our Hamiltonian matrix has the form:

$$H = \begin{pmatrix} \langle +|\,\hat{H}\,|+\rangle & \langle +|\,\hat{H}\,|-\rangle \\ \langle -|\,\hat{H}\,|+\rangle & \langle -|\,\hat{H}\,|-\rangle \end{pmatrix} = \begin{pmatrix} a+b & c \\ c & a-b \end{pmatrix} \tag{A5}$$

Setting $det(H - E) = 0$ we find the eigenvalue equation $E^2 - 2aE + a^2 - b^2 - c^2 = 0$, which may be solved using the quadratic formula. This yields $E = a \pm \sqrt{b^2 + c^2}$ from which the Breit-Rabi formula follows after some trivial cancellations.

Appendix B: Rabi Flopping Matrix Elements

In this section, we calculate Ω for the $|2,2\rangle \to |1,1\rangle$ transition as an illustration of how similar matrix elements may be found. We may expand $|F, m_F\rangle$ states in terms of $|m_I, m_S\rangle$ states in the usual fashion, that is, by introducing an identity operator $\sum |m_I, m_S\rangle \langle m_I, m_S|$ to the right hand side:

$$\begin{aligned} |2,2\rangle_F &= |{}^3\!/_2, {}^1\!/_2\rangle \langle {}^3\!/_2, {}^1\!/_2 | 2,2\rangle_F \\ &= |{}^3\!/_2, {}^1\!/_2\rangle \qquad \text{(B1)} \\ |1,1\rangle_F &= |{}^3\!/_2, -{}^1\!/_2\rangle \langle {}^3\!/_2, -{}^1\!/_2 | 1,1\rangle_F \\ &\quad + |{}^1\!/_2, {}^1\!/_2\rangle \langle {}^1\!/_2, {}^1\!/_2 | 1,1\rangle_F \\ &= \sqrt{\frac{3}{4}}\, |{}^3\!/_2, -{}^1\!/_2\rangle - \frac{1}{2}\, |{}^1\!/_2, {}^1\!/_2\rangle \qquad \text{(B2)} \end{aligned}$$

where an F subscript denotes the $|F, m_F\rangle$ basis, and $|m_I, m_S\rangle$ is implied otherwise. Inner products in the above equations are Clebsch-Gordan coefficients [5, p. 188], which are zero when $m_F \neq m_I + m_S$, hence there only being one or two terms in each expansion. Next, we note that to calculate $\hat{I}_x\,|m_I\rangle$ or $\hat{S}_x\,|m_S\rangle$, we must use the property that $\hat{Q}_x = \frac{1}{2}(\hat{Q}_+ + \hat{Q}_-)$, recalling the properties of $\hat{Q}_\pm$ as mentioned in appendix A:

$$\begin{aligned} \Omega &= \frac{\mu_B B^{mw}}{2\hbar} \langle {}^3\!/_2, {}^1\!/_2 | \left[g_I(\hat{I}_+ + \hat{I}_-) + g_S(\hat{S}_+ + \hat{S}_-) \right] \\ &\quad \times \left[\sqrt{\frac{3}{4}}\, |{}^3\!/_2, -{}^1\!/_2\rangle - \frac{1}{2}\, |{}^1\!/_2, {}^1\!/_2\rangle \right] \\ &= \frac{\mu_B B^{mw}}{2\hbar} \frac{\sqrt{3}}{2} (g_S - g_I) \qquad \text{(B3)} \\ &\approx (7.62853 \cdot 10^{10}\text{Hz/T}) \mu_B B^{mw} \qquad \text{(B4)} \end{aligned}$$

We have used the values $g_S \approx 2.00319, g_I \approx -0.000995$. Most of the terms in the above calculation cancel by the orthonormality relation $\langle m_I, m_S | m_I', m_S' \rangle = \delta_{m_I, m_I'} \delta_{m_S, m_S'}$.

[1] H. K. Onnes. The resistance of pure mercury at helium temperatures. *Commun. Phys. Lab. Univ. Leiden*, 12, 1911.

[2] M. H. Anderson, J. R. Ensher, M. R. Matthews, C. E. Wieman, and E. A. Cornell. Observation of Bose-Einstein Condensation in a Dilute Atomic Vapor. *Science*, 269(5221):198–201, 1995.

[3] H.J. Metcalf and P. van der Straten. *Laser Cooling and Trapping*. Graduate Texts in Contemporary Physics. Springer New York, 2001.

[4] Claude Cohen-Tannoudji and William D. Phillips. New mechanisms for laser cooling. *Physics Today*, 43(10):33, 1990.

[5] D.J. Griffiths. *Introduction to Quantum Mechanics*. Pearson international edition. Pearson Prentice Hall, 2005.

[6] E. Majorana. Atomi orientati in campo magnetico variabile. *Il Nuovo Cimento*, 9:43–50, 1932.

[7] Wolfgang Petrich, Michael H. Anderson, Jason R. Ensher, and Eric A. Cornell. Stable, tightly confining magnetic trap for evaporative cooling of neutral atoms. *Phys. Rev. Lett.*, 74:3352–3355, Apr 1995.

[8] Rudolf Grimm, Matthias Weidemller, and Yurii B. Ovchinnikov. Optical dipole traps for neutral atoms. volume 42 of *Advances In Atomic, Molecular, and Optical Physics*, pages 95 – 170. Academic Press, 2000.

[9] J.J. Sakurai. *Modern Quantum Mechanics*. Addison-Wesley, 1994.

[10] B.H. Bransden and C.J. Joachain. *Quantum Mechanics*. Prentice Hall, 2000.

[11] Daniel A. Steck, Rubidium 87 D Line Data, available online at http://steck.us/alkalidata (revision 2.0.1, 2 May 2008).

[12] Ian D. Leroux. Manipulation of ultra-cold atoms using radio-frequency and microwave radiation. unpublished thesis, 2005.

[13] Claude Cohen-Tannoudji, Jacques Dupont-Roc, and Gilbert Grynberg. *Atom-photon interactions: basic processes and applications*. New York : J. Wiley, 1992.

[14] William Happer. Optical pumping. *Rev. Mod. Phys.*, 44:169–249, Apr 1972.

[15] W. Ketterle and N.J. Van Druten. Evaporative cooling of trapped atoms. *Advances in Atomic, Molecular, and Optical Physics*, pages 181–236, 1996.